A method for linking field-surveyed and aerial-detected single trees using cross correlation of position images and the optimization of weighted tree list graphs

Kenneth Olofsson[1], Eva Lindberg[1] & Johan Holmgren[1]

[1]Remote Sensing Laboratory, Department of Forest Resource Management, Swedish University of Agricultural Sciences, kenneth.olofsson@srh.slu.se, eva.lindberg@srh.slu.se, johan.holmgren@srh.slu.se

Abstract

With the present number of forestry remote sensing and field plot survey methods several data sources can be combined to potentially achieve a higher accuracy than with a single data source. Some of these datasets contain single tree information and it would be of great value when designing survey techniques if one could automatically link data from different sources belonging to the same tree. In this paper such a method for linking field-surveyed and aerial detected trees is described and evaluated. A simulation study and experimental data show the accuracy of the algorithm at different settings. The method correctly links >90 % of the trees if the corresponding datasets have a position error standard deviation of 1 [m] and 10 % omission and commission errors.

Keywords: LiDAR, digital aerial images, data fusion, field plots, single tree detection and linking.

1. Introduction

New remote sensing technology allows for high precision measurements of vegetation. Low resolution airborne laser scanner (ALS) data can be used to establish statistical models for the prediction of biophysical properties, *e.g.* stem volume and mean tree height, on a raster cell level (*e.g.* Means *et al*. 2000; Næsset 2002). In high resolution ALS data, individual trees are identified which makes it possible to establish statistical models on the tree level (*e.g.*, Hyyppä *et al.* 2001; Persson *et al*. 2002; Solberg *et al*. 2006). The size of the random errors for statistical models will become a problem if there is a poor co-registration of field surveyed data and remote sensing data and this will affect the quality of remote sensing based forest inventories. High precision position measurements can be achieved with advanced GPS equipment but only below a clear sky where no canopy obscures the satellite signal. The GPS errors will be large within a forest stand with a high basal area (Næsset and Jonmeister 2002). Thus there is a need for an automatic tree linking algorithm that rectifies poorly registered coordinates in raw data. This paper presents a method for the automatic co-registration of field surveyed and remotely sensed data. The performance of the method was tested by using simulations. The algorithm was tested empirically in a forest in west Sweden.

2. Method

Linking field surveyed and aerial detected trees requires input data from a remote sensing single tree detection method (*e.g.*, Gougeon, 1995; Holmgren and Wallerman 2006; Hyyppä *et al*. 2001; Korpela 2004; Persson *et al*. 2002; Pinz, A., 1989; Pollock 1996; Solberg *et al*. 2006). In the empirical study in this paper the ALS single tree detection method developed by Holmgren and Wallerman (2006) has been used. Single tree data collected from a field plot is also necessary.

The method for linking field surveyed and aerial detected single trees is a two stage process: first, the field plot coordinate-system is rectified to the aerial data coordinate-system, and second, the field surveyed trees within the plot are linked to the most probable candidates of the aerial detected trees positioned nearby.

2.1 Field data

The study area is located in the west of Sweden (lat. 60^0 43' N, long. 15^0 10' E). The dominating tree species are Norway spruce (*Picea Abies*), birch (*Betula spp*) and Scots pine (*Pinus Silvestris*). Field reference data was collected in 155 field plots with 10 m radius each. The position of the field plots were measured using a Global Navigation Satellite System (GNSS). Within the plots, all trees with a stem diameter larger than 50 mm were callipered and tree species was recorded. The positions of the trees were registered relative to the centre of each plot by measuring azimuth and distance.

2.2 ALS data

The laser data was acquired using an Optech scanner with a scan density of approximately 10 points/m^2. The flying height was 900 m, the pulse repetition rate 100 kHz and the field of view 34^0. The ALS single tree detection method used is developed by (Holmgren and Wallerman 2006).

2.3 Rectifying the field plot coordinate system

Usually field plot measured tree positions have good precision but lower accuracy. The data is biased. Therefore, the two coordinate systems need to be rectified before the field plot trees can be linked to the aerial detected trees. The algorithm in this study uses an estimated position of the field plot centre to start the search, and a search area that contains the real field plot centre. The search area is set depending on the expected bias error in the experimental setup. From the start position, aerial single tree data from within the search area is collected as a list. This list must contain the tree position coordinates, x and y, and a variable that represents the tree size, *e.g.* the tree height, H, or the crown diameter, D. In this study the tree height was used. For the field plots a similar list is required with the positions of the trees and a size variable. In this study the stem diameter at breast height, *DBH*, was chosen to represent the size of the tree.

The tree lists are used to create two single tree position images, figure 1. Within the image, each tree is displayed as a Gaussian surface where the x and y coordinates determine the position within the image, the tree size variable determines the amplitude of the Gaussian function, and the standard deviation is set to the expected tree position precision, figures 1 and 2. Since large trees often are detected from above whereas small trees often are hidden, the maximum surface is used; from all of the Gaussian functions that cover the same area, the highest value is chosen, figure 2.

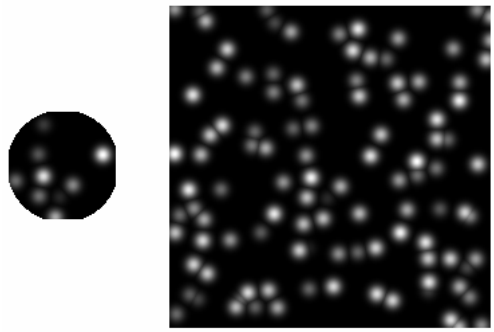

Figure 1: Two single tree position images where each tree is modelled as a Gaussian surface with the amplitude proportional to the tree size and the standard deviation equal to the radial position error. LEFT: The position image of a circular field plot where the stem diameter at breast height is used as amplitude. RIGHT: The position image of an area with aerial detected trees, with the tree height as amplitude.

The two single tree position images are then cross correlated to find the closest match between the patterns in the two images. The field plot image can be rotated a few degrees between each correlation run, in order to compensate for possible compass errors. The normalized correlation coefficient, *cc* (Gonzalez and Wintz, 1987) is defined as:

$$cc(m,n)=\frac{\sum_x \sum_y \left[g(x,y)-\bar{g}(x,y)\right]\left[k(x-m,y-n)-\bar{k}\right]}{\sqrt{\sum_x \sum_y \left[g(x,y)-\bar{g}(x,y)\right]^2 \sum_x \sum_y \left[k(x-m,y-n)-\bar{k}\right]^2}} \quad (1)$$

where g is the aerial position image, k is the field plot position image, $\bar{k}$ is the average intensity of k and $\bar{g}\,(x,y)$ is the average intensity of g of the region coincident with $k(x,y)$. The position and rotation with the highest correlation coefficient, equation 1, is assumed to be the place where the real field plot center is located. The greater the position image resolution results in the higher accuracy of the field plot matching achieved.

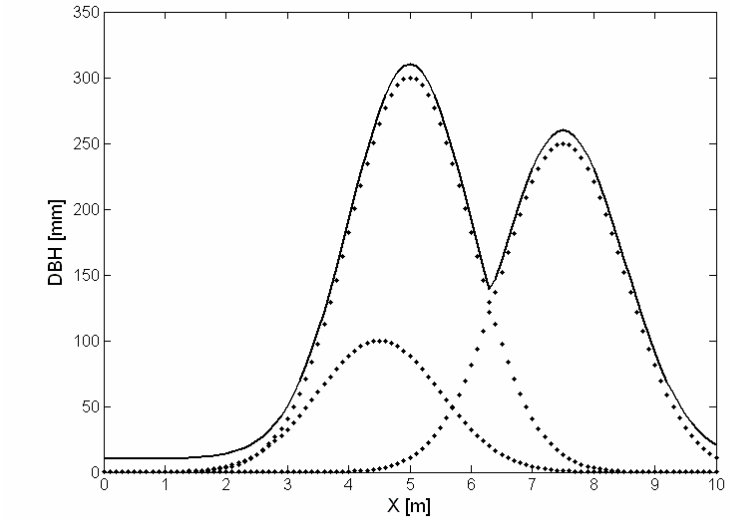

Figure 2: [DOTTED CURVES]: Three field plot trees with a stem diameter at breast height (DBH) of 100, 300, and 250 [mm] and positions in the x-direction of 4.5, 5 and 7.5 [m], displayed as Gaussian functions with the DBH as amplitude and the position error (1 [m]) as standard deviation. [SOLID CURVE]: The maximum surface of all trees in the plot.

2.4 Linking field surveyed and aerial detected trees

The algorithm uses the tree heights for both the aerial detected trees and the field surveyed trees. If the tree height is not sampled by the single tree detection method or the field survey – if for instance the crown diameter and the *DBH* is used instead – the tree heights must be estimated from the size parameters used. In order to get an estimate of the tree height, when the information is missing, a regression function from an area with similar climate and similar forest types is necessary. These size parameters to tree height functions can be pre-calculated in a database or curve fitted prior to a large scale experiment. In this study the single tree detection method samples the tree height directly but the field survey only samples the *DBH*. The field tree heights were estimated by a hyperbolic tangent function:

$$H = C * \tanh(p * DBH) \tag{2}$$

where *C* is the tree height amplitude parameter and p is the tree height phase parameter. *C* and *p* were estimated by a non linear regression of data from forest areas similar to the one used in the experiment.

For every field surveyed tree the algorithm calculates the radial ground distance, *r*, and the normalized Euclidian distance of the tree tops, *d'*:

$$d' = \sqrt{\left(\frac{r}{\sigma_r}\right)^2 + \left(\frac{H_{aerial} - H_{field}}{\sigma_h}\right)^2} \tag{3}$$

where H_{aerial} is the height of the aerial detected tree, H_{field} is the height of the field surveyed tree, σ_r is the estimated radial error and σ_h is the estimated height error, figure 3. To limit the size of the calculation only aerial detected trees close to field trees are used. The largest distance to accept an aerial tree is defined as:

$$rAccept = b + f * DBH \tag{4}$$

where the parameters *b* and *f* should be set to include a reasonable number of trees. All aerial trees inside this radius are added to a list of tree links. To get an indication of how good a link is, a weight based on the normalized Euclidian distance of the tree tops is set to every tree link:

$$w = \frac{1}{(d'+1)^2} \tag{5}$$

The weight is higher the closer the linked trees are; a zero tree top distance gives a weight of one.

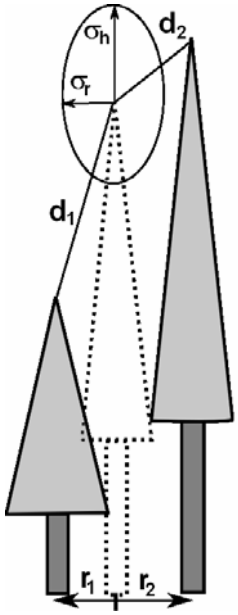

Figure 3: Two field plot trees (gray) with possible links to an aerial detected tree (dotted lines) with position and height errors. The tree top distances d1 and d2, the radial distances r1 and r2, the height error standard deviation σh and the radial error standard deviation σr, are used by the linking algorithm to determine which tree to choose.

In the tree link list the algorithm then searches for connected tree clusters, *i.e*. a group of field surveyed and aerial detected trees that are linked together. Each link only contains one field surveyed tree and one aerial detected tree, but since each field tree can be linked to several aerial trees and each aerial detected tree can be linked to several field trees, a network of connections can become a cluster of trees – a tree list graph.

Since every field surveyed tree should only be connected to one aerial detected tree, multiple links must be removed from the list. The algorithm solves this by trying every possible combination of links in a tree cluster. Combinations with multiple links are discarded. The link combination with the highest sum of weights is the solution that is chosen for each tree cluster. All other links are removed from the list. This brute force method can be time consuming if the tree clusters are large and therefore the problem was minimized by only trying aerial detected trees standing close to a field surveyed tree.

2.5 Simulations

To get an estimate of how well the method works, the matching and linking algorithm were applied to 1125 simulated field plots.

2.5.1 Generating simulated trees

In order to have a realistic virtual tree lists, distribution generating functions were curve fitted from the field data. The relative frequency distributions of the *DBH* were modelled by two-parameter Weibull functions, *f(DBH; k,λ)*, for the three dominating species: pine, spruce and birch; equation 6.

$$f(DBH;k,\lambda)=\frac{k}{\lambda}\left(\frac{DBH}{\lambda}\right)^{k-1}e^{-(DBH/\lambda)^k} \qquad (6)$$

The simulated field tree *DBH* to height curves were modelled as hyperbolic tangent functions, equation 2, with added residuals calculated from a Gaussian distribution with standard deviations also modelled as hyperbolic tangent functions, equation 7,

$$\sigma_H = C\text{residual} \cdot \tanh\left(p\text{Residual} \cdot DBH\right) \quad (7)$$

where σ_H is the simulated field tree height standard deviation, *DBH* is the field surveyed stem diameter at breast height, $C_{residual}$ is the tree height residual amplitude parameter and $p_{Residual}$ is the tree height residual phase parameter. The settings for the distribution generating functions are shown in table 1.

Table 1: Simulation settings for the different tree species: the scale and shape parameter for equations 6, the C and p parameters for equation 2 and the Cresidual and pResidual parameters for equation 7.

	Pine	Spruce	Birch
k, scale	286.0	252.0	206.0
λ, shape	2.69	2.46	2.77
C	24.0	28.0	22.0
P	0.0042	0.0035	0.0075
CResidual	3	2.7	1.8
pResidual	0.01	0.01	0.01

Since the field surveyed data had an approximate ratio of 45 % pine, 45 % spruce and 10 % birch this setting was chosen for the simulation. When generating a tree, the function first chooses a species. Then a *DBH* is generated from equation 6 with parameters corresponding to the chosen species. Finally the tree height is calculated from equation 2; with a residual calculated from equation 7.

2.5.2 Simulation of field plot and aerial single tree data

To create a field plot, the algorithm was used to add trees, until the correct number of trees per hectare (*SPH*) was achieved. The stem diameter at breast height was saved as field data and the tree height was saved as aerial data. The position was saved in both the aerial and the field data. To simulate position errors the coordinates of the aerial data was translated in a random direction in the ground plane, with a radial magnitude generated by a Gaussian distribution. If the tree crowns (modelled as ellipsoids of revolution) of two specimens were intertwined (had a cross section radius overlap of more than 30 % of the distance between the trees) the algorithm discarded the solution and tried a new tree. If the tree had a *DBH* < 50 mm it was discarded since the field plot sampling had 50 mm as a lower size limit. To get the correct number of omissions, some of the trees were not saved in the aerial data, and to get the correct number of commissions some trees were added only to the aerial data. To get a larger search area, trees outside of the field plot were added to the aerial data. Each tree in the field data and aerial data had a label to make it possible to identify a correct link. The simulation was run with three different numbers of stems per hectare (*SPH*), 300, 600 and 900; with five different position error standard deviations, 0, 0.5, 1, 1.5 and 2.0; and with three combinations of commission and omission errors, 0/0, 10/10 and 20/20 %. For each setting 25 plots were tested giving a total of 1125 plots in the simulation. The field plot radius was set to 10 m for all plots.

2.5.3 Configuration of the software

In order not to use the same field plot data for both the simulation and for the *DBH*-height estimate in the field plot matching software, forest data from other areas in the same climate zone was used to calibrate the algorithm. The parameters *C* and *p* in table 2 was estimated this

way. The other parameters were set to values estimated to be feasible in an inventory of a real forest.

Table 2: The settings of the configuration file for the software. A = size of search area, Δθ = field plot rotation angle increment, min/max θ = field plot rotation end values, b = tree position search bias, eq 4, f = tree position search factor, eq 4. C = tree height estimation amplitude parameter eq 2, p = tree height estimation phase parameter, eq 2. σh = height residual error, σr =ground distance radial error. mpp = correlation image resolution.

A	Δθ	min / max θ	b	f	C	p	σ_r	σ_h	mpp
[m^2]	[°]	[°]	[m]	[m]/[mm]	[m]	1/[mm]	[m]	[m]	[m]/pixel
3600	2	±16	1.5	0.002	25.5	0.0036	1.0	3.0	0.5

2.6 Empirical tests

To support the simulation study a small empirical test was performed. In this test the trees did not have labels as in the simulation study so the number of correct links were not possible to achieve but it was possible to see if the method had a high connection rate. That is, if it managed to connect all the trees in the plot. This would be difficult if the tree position patterns differed too much between the field plot and the aerial data. It was also possible to see if the rectified field plot coordinate systems had a large bias and a large compass error. Since the field plot centres were measured using a Global Navigation Satellite System (GNSS) the expected bias and compass error was small. However if the found plot is not the correct one, any compass direction and bias within the search space is equally possible. Therefore small bias and compass errors indicate that the true field plots have been located.

The field plot matching algorithm was applied to the material both for original field data coordinates and for data where the coordinates of each tree had been deliberately displaced 60 m, in order to have two datasets: one set containing field plots and one set not containing any field plots. The proportion of connected trees for each aerial detected tree within the plot and the average bias of the field plots were calculated for different search area sizes and field plot rotation.

3. Results

3.1 Simulation results

Results from the simulation show that the method has a high connection rate if the position radial error standard deviations are 1 [m] or smaller, figure 6. Even with as high omission and commission errors as 20 % the method still links more than 70 % of the trees correctly. When the position errors increase, the connection rate decreases, especially for dense forests and a single tree detection method with large omission and commission errors.

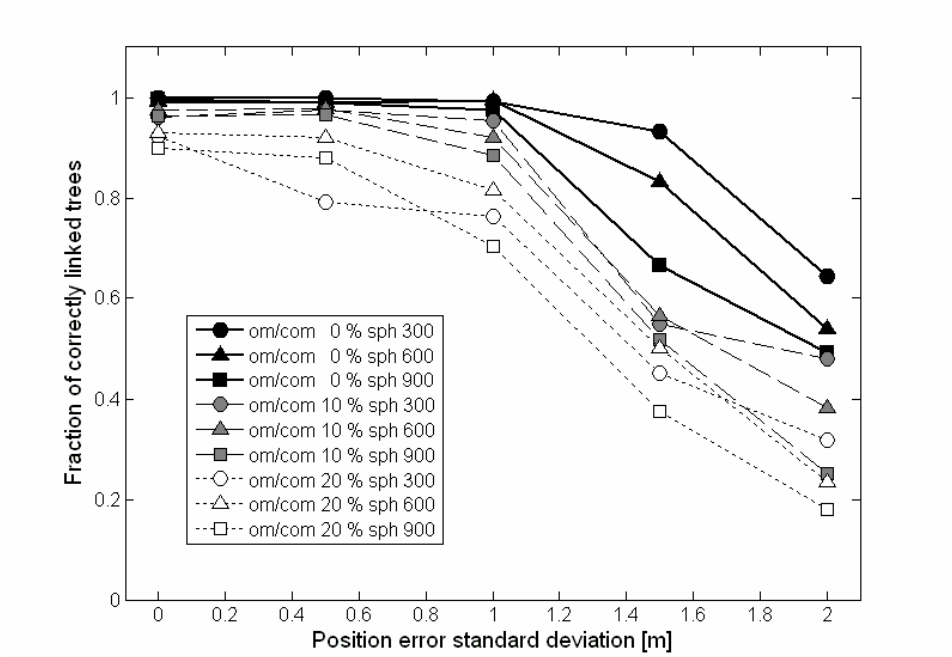

Figure 4: Simulation of the expected amount of correct links between field trees and aerial detected single trees for 300, 600 and 900 stems per hectare, 0, 10 and 20 % omission and commission errors, and 0.0, 0.5, 1.0, 1.5 and 2.0 [m] radial position error standard deviations.

3.2 Results empirical test

Table 3 shows the results of the empirical tests for different search area sizes and field plot rotation, both for search areas containing field plots and for search areas without field plots.

Table 3: The results for the empirical test of the automatic tree linking algorithm

	Search areas with field plots	Search areas without field plots	Search areas with field plots	Search areas without field plots	Search areas with field plots	Search areas without field plots
Search area [m^2]	1600	1600	3600	3600	10000	10000
Min/max compass search angles [deg]	±8	±8	±16	±16	±16	±16
Proportion of connected aerial trees	92.9%	76.9%	93.1%	79.5%	93.5%	84.5%
Average field plot radial bias displacement [m]	1.68	7.94	3.06	15.81	5.42	31.83
Average compass angular displacement [deg] (absolute values)	2.23	5.56	2.95	9.14	3.24	7.96

Table 3 shows that the search areas with field plots have a higher connection rate than the search areas without field plots. That is they connect more trees even though they are not necessarily the correct ones as indicated in the simulation study. In the case with the search areas without

field plots of course none of the tree links are correct. The radial displacements and the compass shifts are also fairly small and constant for the search areas containing field plots whereas for the search areas without field plots the displacements increase with increasing search area, indicating that the algorithm manages to find a field plot if it is present in the search space.

4. Discussion and conclusions

A new method for automatically linking of field-surveyed and aerial-detected individual trees was implemented and tested by using simulations and an empirical field data set with high accuracy GPS measurements. The method could be used for any remote sensing method that produces a map with tree positions and relative tree sizes. The simulation results show that a high proportion of correctly linked trees can be obtained if the chosen single tree detection method has a small tree position random error (≤1m standard deviation) and less than 20 % commission and omission errors. With a higher random error of the tree positions the performance of the method will become more affected by a greater omission and commission error. The empirical results also indicate that the algorithm manages to find and connect trees in a field plot if it is present in the search space.

Acknowledgements

The research of this study was founded by Formas (www.formas.se). The field data and airborne laser scanner data was financed by the Swedish Forest Agency.

References

Gonzalez, R. C. and Wintz, P., 1987. Digital Image Processing. Second edition. Addison-Wesley Publishing Company. ISBN 0-201-11026-1. correlation coefficient: equation (8.4-4), pp. 426.

Gougeon, F. A. 1995. A crown-following approach to the automatic delineation of individual tree crowns in high spatial resolution aerial images. *Canadian Journal of Forest Research, 21*, 274-284.

Holmgren, J. and Wallerman, J., 2006. Estimation of tree size distribution by combining vertical and horizontal distribution of LIDAR measurements with extraction of individual trees. In: T. Koukal and W. Schneider (Eds.). Proceddings from Workshop on 3D Remote Sensing in Forestry, Vienna, Austria, 14-15 February 2006, pp. 168-173. University of Natural Resources and Applied Life Science, Vienna, Austria.

Hyyppä, J., Kelle, O., Lehikoinen, M. and Inkinen, M., 2001. A segmentation-based method to retrieve stem volume estimates from 3-D tree height models produced by laser scanners. *IEEE Transactions on Geoscience and Remote Sensing*, 39, 969-975.

Korpela, I. 2004. Individual Tree Measurements by Means of Digital Aerial Photogrammetry. (Doctoral dissertation. The Finnish Society of Forest Science, The Finnish Forest Research Institute). SILVA FENNICA Monographs 3-2004.

Means, J. E., Acker, S. A., Brandon, J. F., Renslow, M., Emerson, L. and Hendrix, C. J., 2000. Predicting forest stand characteristics with airborne scanning lidar. *Photogram. Eng. Remote Sensing*, 66, 1367-1371.

Næsset, E., 2002. Predicting forest stand characteristics with airborne scanning laser using a practical two-stage procedure and field data. *Remote Sens. Environ*., 80, 88-99.

Næsset, E. and Jonmeister, T., 2002. Assesing point accurcy of DGPS under forest canopy before data acqusition, in the field, and after processing. *Scandinavian Journal of Forest Research*, 17:4, 351-358.

Persson, Å., Holmgren, J. and Söderman, U., 2002. Detecting and measuring individual trees using an airborne laser scanner. Photogram. Eng. Remote Sensing, 68, 925-932.

Pinz, A., 1989. Final results of the vision expert system VES: finding trees in aerial photographs, in *Wissensbasierte Masterkennung. (Knowledeg-based pattern recognition.) OCG - Schriftenreiche* 49, pp 90-111. Oldensbourg Verlag.

Pollock, R. J. 1996. The automatic recognition of individual trees in aerial images of forests based on a synthetic tree crown image model. Unpublished doctoral dissertation. The University of British Columbia, Vancouver, B. C.

Solberg, S., Næsset, E. and Bollandsås, O. M., 2006. Single tree segmentation using airborne laser scanner data in a heterogeneous spruce forest. *Photogram. Eng. Remote Sensing*, 72, 1369-1378.